Science and Technology for Energy Transition **79**, 74 (2024)

https://doi.org/10.2516/stet/2024082

Available online at:
stet-review.org

Emerging Advances in Hybrid Renewable Energy Systems and Integration
Muhammad Zakarya, Santosh Tirunagari, Jinguang Han and Peiying Zhang (Guest Editors)

REGULAR ARTICLE OPEN ACCESS

A novel hybrid coil design and implementation for wireless power transfer systems

Ali Pashaei[1,*], Emrullah Aydin[2], Mehmet Akif Ozdemir[3], Yusuf Kosesoy[4], and Mehmet Timur Aydemir[5]

[1] Computer Engineering, Faculty of Engineering and Natural Science, Istanbul Rumeli University, Istanbul, 34020, Turkey
[2] Electric-Electronic Engineering, Faculty of Engineering and Natural Science, Malatya Turgut Ozal University, Malatya, 44050, Turkey
[3] Electric-Electronic Engineering, Faculty of Engineering, Gazi University, Ankara, 06080, Turkey
[4] Electrical Engineering, Faculty of Engineering, Eindhoven University of Technology, Eindhoven, 2613 BD, The Netherlands
[5] Electric-Electronic Engineering, Faculty of Engineering and Natural Science, Kadir Has University, Istanbul, 34020, Turkey

Received: 10 July 2024 / Accepted: 6 September 2024

Abstract. Wireless Power Transfer (WPT) has been drawing a lot of attention in the last ten years parallel with the market increase in electric vehicles. Although conductive charging methods are still the preferred ones, WPT-based charging systems are used as clean and flexible alternatives. At the center of these systems are the transmitting and receiving coils, and different coil types have been proposed in the literature. This study proposes a square-hexagonal hybrid coil structure to increase magnetic coupling by shaping the magnetic field. In addition, this design aims to minimize the coupling coefficient variation for misaligned coils which is one of the most significant problems in WPT systems. A 3D model of the coils was created and analyzed using ANSYS, Maxwell software. Compared to the conventional square coil structure the coupling coefficient of the proposed structure is less affected by misalignment on the x and y axes, and as a result, it has a better efficiency. In addition, a WPT system operating at 50 W, 85-kHz is designed and tested in a laboratory environment. The FEA analyses and experimental application results largely overlap, and accordingly, the coil-to-coil efficiency of our WPT system was 93.5% and the overall efficiency of the system was 87%.

Keywords: Wireless power transfer, Coil design, Electrical vehicles, Misalignment.

1 Introduction

The transfer of contactless energy through an air gap is called wireless power transfer (WPT). Because this method is clean and reliable, it has been proposed for various applications including electric vehicle battery charging. Tesla demonstrated the transfer of electrical power from an air gap via magnetic coupling in the 1890s. Wireless power transfer studies gained momentum in 1994 when researchers designed a 60 kW wireless charger that powered a passenger bus in different modes [1]. The reported efficiency was approximately 60% at 60 kW output power for both operating modes. Because high-power transistors operate in a limited range, the switching frequency is limited to 400 Hz. In 1994, Boys [2] developed an inductive power transfer system. The WPT prototype was operated at 10 kHz at a 500 W output power level.

Research groups have been working on wireless EV charging from Georgia Tech, New York, Virginia Tech, Utah State, and other universities [3]. A 4 kW WPT charger developed and designed an asymmetric coupler to protect the coupling coefficient from the air gap and misalignment changes, based on research from Virginia Tech [4]. A new device for charging different electric car models was designed by Georgia Tech researchers [5]. Research from New York University has worked on a multilevel polyphase resonant converter for WPT [6]. The Utah State's University Power Electronics Laboratory is implementing a mobile wireless charger project for electric vehicles and evaluating its environmental and economic applicability [7]. WPT technology for stationary and portable charging was developed by Oak Ridge National Laboratory (ORNL) [8]. They evaluated the wireless power transfer technology from many perspectives. The most important of these are EM exposure to the human body, power flow control, converter design, and standardization of the WPT [9, 10].

In WPT design studies, issues such as the correct coil structure, resonance frequency, power level, and selection of compensation structure have been discussed. Coils play

* Corresponding author: ali.pasaoglu@rumeli.edu.tr

an important role in WPT because they employ electrical energy to create a magnetic flux that enables power transfer without any electrical connection. Coils are classified into two types: non-polarized (NPPs) and polarized (PPs) pads. PPs are multiple coil windings (including DD, DDQ, and BP) that can generate both parallel and vertical fluxes. NPPs are single coil windings that can produce only the vertical components of the flow. Circular, square, rectangular, pentagonal, and hexagonal coil structures can be classified under the NPPs category. Circular coils are more frequently used than other structures. Square and rectangular structures are suitable for perfectly aligned edges. Because such coils have sharp corner edges, eddy currents are produced and the impedance and inductance values increase. Rectangular coils show more tolerance to misalignment than circular and square coil structures. In [11], rectangular, circular, and hexagonal coil structures were compared based according to their misalignment states. According to the results obtained, the hexagonal winding structure gives the best results in perfectly aligned conditions and can transmit maximum power in this case. However, it was observed that the rectangular structure yielded better results when the misalignment ranged from 0 mm to 400 mm [11].

Owing to the poor performance of NPPs in horizontal alignment, multi-shape coils (PPs) have been proposed. These shaped coils are suitable for both single and three-phase applications. The most frequently proposed PP structures are the DD, DDQ, QDQ, and bipolar BP. Among these coil structures, the QDQ coil structure exhibits the best results concerning misalignment, but its disadvantage is that it is suitable for low- power models [12]. The coil structure is defined as the QDQ coil four circular coils surrounded by a rectangular coil structure. The system exhibits 91.8% efficiency at a misalignment of 0 cm and 78% at a 15 cm misalignment. The Double D polarized pads consist of two square or rectangular coils. This coil model can produce a flux in only one direction. The advantage of this structure is that the amount of leakage flux at the edge corners is low, and it can cover the horizontal and vertical magnetic fluxes. This pad may be suitable for transmitting coils in dynamic and stationary applications because it provides better results in the case of misalignment [13]. The DDQ coil is a different version of the DD coil and is, capable of producing approximately twice as much magnetic flux as a circular coil structure. The DD and Q coils can be used together to improve lateral alignment problems. It is a good choice as a receiver pad because of its ability to capture all types of magnetic flux vectors [14, 15].

Bipolar (BP) pads are composed of coils that are similar in size. The most important advantage of BP pads over DDQ pads is their high cost. Approximately 25% to 30% less copper was used in these coils. Researchers tested a 2-kW WPT system and compared rectangular and circular coils in the case of angular misalignment. The results show that circular pads are more efficient [16, 17]. Another study compared the flux coupling between rectangular and circular coils and concluded that circular coils showed better results than rectangular coils [18]. It has been observed that the magnetic flux height is low in circular coils. A solenoid coil structure for solving the magnetic flux problem in circular coils was proposed in [19]. In the design of a 3 kW wireless charging system, researchers reported a good tolerance (±200 mm) for lateral misalignments with an air gap of 200 mm. The efficiency of this system has been reported to be 90% [20]. In [21], a quad coil structure was proposed where the losses and leakages were very low and flux production was twice that of a circular coil structure. Bipolar coils are used and analyzed for three-phase WPT systems [22]. In the aligned mode, the system transmits 50 kW over a 150 mm air gap with a DC-DC transmission efficiency of 95%. The authors in [23] proposed a pentagonal coil structure that is claimed to be less affected by the air gap change compared to circular and square coils. In [24], the authors proposed a hexagonal coil structure with 7.7 kW power and 85 kHz frequency. A structure with a system efficiency of 96.5% is more convenient and has lower weight compared to circular coils however great care must be taken in the manufacture of this coil structure.

In this study, a square-hexagonal hybrid coil structure was proposed. The designed coil was compared with the square coil using FEA for both designs. For comparison, the effect of the air gap change on the coupling coefficient was examined when the coils were perfectly aligned. Then, the change in the coupling coefficient was observed with respect to the misalignment in the x-axis, y-axis, and both axes while the air gap of the coils was fixed. To observe the performance of the proposed coil design with a power electronic circuit, a simulation was performed using ANSYS Simplorer software. To demonstrate the accuracy of the simulation results, a 50-W WPT system was implemented in the laboratory and the experimental results were obtained.

2 Fundamentals of WPT systems

2.1 Basic theory of wireless power transfer

These two laws are used to mathematically explain how power is transmitted inductively. According to Ampere's circuit law, the integral of the magnetic field strength in a closed area is equal to the net electric current flow in the closed area [25].

$$\nabla \times \vec{H} = \vec{J} \leftrightarrow \oint \vec{H}.dl = \int \vec{J}.\vec{ds} = I_K \tag{1}$$

where J is the current density [A/m^2], I_K is the net current through the region bounded by the closed path [A], H is the magnetic field strength [A/m]. Faraday's law can be written as:

$$\nabla \times \vec{E} = -\frac{\partial \vec{B}}{\partial t} \leftrightarrow \oint \vec{E}.dl = -\frac{d}{dt}\int \vec{B}\,dA = emf \tag{2}$$

where $\vec{E}$ the electric field [V/m], $\vec{B}$ is the magnetic flux density [T], and A is the area [m^2]. Mathematically, the magnetic flux can be described as follows [25].

$$\phi = \int BdA \tag{3}$$

Figure 1 shows the coupling between two simple coils. When current flows from the primary side, magnetic flux

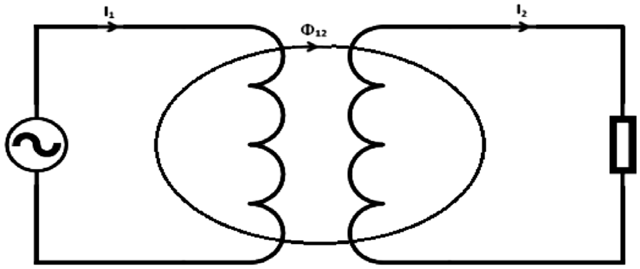

Figure 1. Current and magnetic field formation in the coils.

occurs on the secondary side. If the current is varying over time, the flux induces a voltage on the other side. The two coils were coupled through mutual flux ϕ_{12}.

As the coils are not wound on the same core and the secondary coil is attached to another body in WPT systems, there is always an air gap and it is also possible that the centers of the two coils may not always be aligned resulting in a change in the mutual inductance between the coils. The magnetic field and current are proportional to each other [25]. Therefore, the mutual inductance and magnetic flux are interconnected.

$$M_{12} = \frac{N_1 \phi_{12}}{I_2} \tag{4}$$

In equation (4), the terms $N_{1,}$ I_2 and ϕ_{12} are the turns number for the primary coil, the current induced in the secondary coil, and the mutual flux respectively. The coupling coefficient (k) and mutual inductance (M) are expressed as follows.

$$k = \frac{M}{\sqrt{L_1 L_2}} \tag{5}$$

where L_1 and L_2 are primary and secondary self-inductance.

2.2 Compensation structures for WPT systems

Choosing the correct compensation topology is crucial for WPT systems. While determining the type of compensation topology of the WPT system, the most suitable topology is selected based on the application, power to be transferred, distance between the coils, and operation frequency. After the topology is determined, the capacitance value in the secondary circuit is first selected depending on the operating frequency. The secondary coil is compensated to increase the power transferred to the secondary circuit, whereas the primary circuit is compensated to increase the input power factor in the primary coil. To achieve high efficiency in a wireless power transmission system, we must work on two parameters. These are the coupling factor and quality factor [26]. We have four types of compensation structures.: (SS) [27–29], (SP) [30], (PS) [31] and (PP) [32].

In this study, the SS was chosen as the compensation structure [33]. The SS compensation structure is suitable for EVs because it has two important advantages. First, the capacitor values on the primary and secondary sides are independent of the load conditions and M value. The second advantage is that the impedance reflected in the secondary coil maintains a unity power factor because it does not add an imaginary part to the primary coil. Figure 2 shows the general circuit structure of the SS compensated WPT. C_1 and C_2 are the primary and secondary side capacitors, $Q_1 - Q_4$ are the semiconductor switch elements of the inverter, $D_1 - D_4$ are the secondary side full bridge rectifier switching elements. On the primary side of the WPT general circuit structure, a high-frequency inverter changes the DC voltage to AC voltage. The square wave starts a current flow through the SS resonant circuit and a voltage is induced on the other side.

3 Hybrid square hexagon coil design for WPT systems

Coil geometry plays a very important role in the efficiency of WPT systems. WPT designs use different types of coil shapes such as circular, square, rectangular, pentagonal, hexagonal [34], and hybrid models to improve efficiency and misalignment issues. In this study, the square coil structure and the proposed hybrid square hexagonal coil structure were compared under perfect alignment and misalignment conditions.

The inductance values required for a 50 W WPT system design with 25 V input voltage, 85 kHz operating frequency, and SS compensation topology were calculated in MATLAB using the relevant equations. The primary and secondary coils were identical, the distance between them was 5 cm and the current density reached a maximum of 4 A/mm^2. Parametric optimization procedures were performed using FEA to obtain the mutual and self-inductance values. For a fair comparison of the two coil structures, the outer edge lengths and copper amounts were kept the same. The outer side lengths of the coils were kept equal for the primary and secondary coils; 200 mm for the square part and 80 mm for the hexagonal part.

According to the FEA analysis, the square coil structure should consist of 13 turns, and the square-hexagonal hybrid structure should consist of 16 turns equally divided between the square and hexagonal parts. In this case, the total amount of copper used for the primary and secondary sides of both structures was calculated to be 15.356 mm^3.

To demonstrate the benefits of the proposed coil, square and square-hexagon hybrid coil structures, were analyzed under the same conditions. In Figure 3, three-dimensional (3D) models of the conventional square and proposed square-hexagonal hybrid coil structures are shown.

Another important parameter to be considered in coil design that yields the desired power is the coupling coefficient (k). The effects of variation in the air gap between the sender and receiver coils, and the misalignment when the secondary coil moves in x-axis or y-axis direction on the coupling coefficient were investigated for the two different coil models shown below. Figure 4 shows the results for different air gaps for the alignment of the coils. Figure 5 shows the results for various misalignments in the x-axis whereas the results for the case of simultaneous misalignment exist both on the x-axis and y-axis in Figure 6.

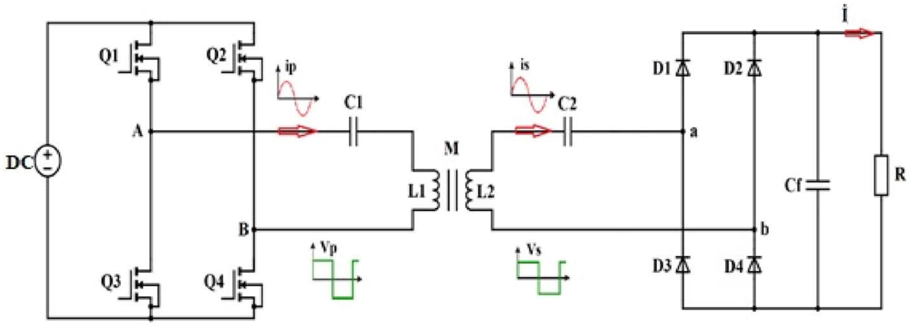

Figure 2. General circuit structure of SS compensated WPT system.

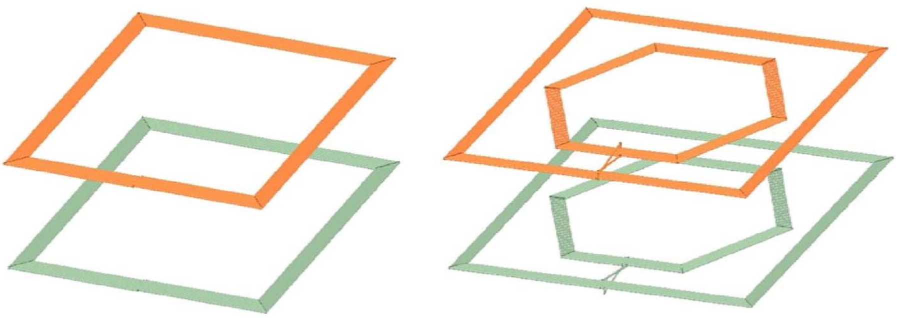

Figure 3. 3D model of square and proposed coil structures.

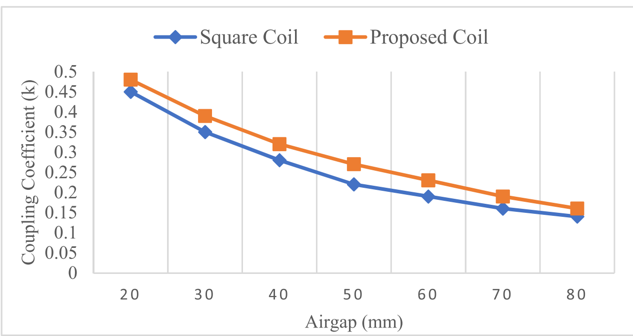

Figure 4. The impression of air gap variation on (k).

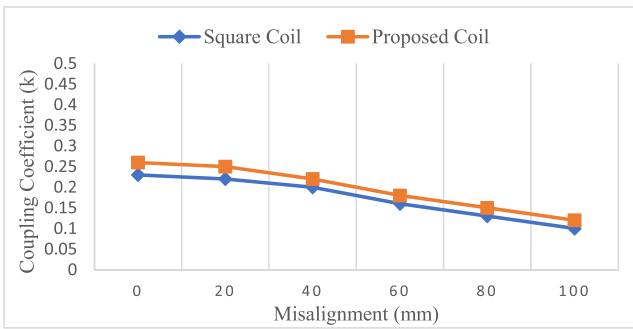

Figure 5. The effect of misalignment in x-axis on (k).

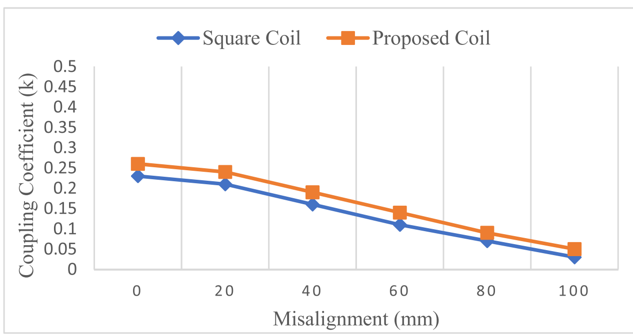

Figure 6. The effect of misalignment in x and y-axis on (k).

The simulation results show that the coupling coefficient values of the proposed coil structure and the conventional square coil structure are 0.27 and 0.23, respectively when the air gap is maintained at 5 cm. This indicated a 17% increase in (k). The benefit of the proposed structure is also clearly observed when there is a misalignment.

Figure 7 shows the magnetic flux density distributions of the simulated structures. The flux is concentrated between the primary and secondary coils in the proposed coil model, whereas it weakens in the central region for the conventional structure.

When the analysis results are examined, it is observed that the proposed coil structure has a better magnetic

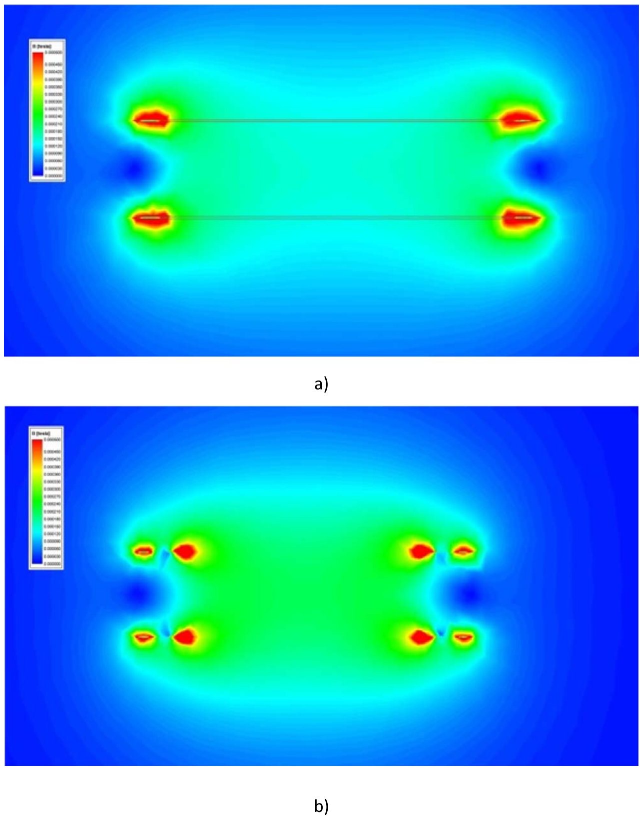

Figure 7. Magnetic flux density distribution of the a) square coils, b) proposed coils.

coupling than the conventional square coil structure. For this reason, a 50-W WPT system was implemented with the proposed coil structure, and its performance is examined in the next section.

4 System design, simulation, and experimental implementation

In this section, the design, simulation, and application of the hybrid square hexagonal coil structure, designed in the previous sections, for a 50-W WPT system are described. The values for the targeted system are listed in Table 1. AWG 38 litz wire with a conductor cross-section of 0.78 mm^2 is used for the coils and the coils manufactured in the laboratory are shown in Figure 8. The L and M values of the produced coils were measured using an LCR meter and compared with the results obtained by FEA. In Table 2, the self and mutual inductance values with FEA and experimental results are compared. The designed system is illustrated in Figure 9. The current and voltage waveforms on both sides are shown in Figure 10.

To prove the accuracy of our FEA and theoretical calculations, an experiment was conducted in a laboratory environment. After the coils were wound, 50 W of power was transferred between the two coils with an air gap of 5 cm. A DC input voltage of 25 V fed the power electronics inverter board. A TMS0F2812 DSP processor was used to generate PWM signals. Figure 11 shows the experimental setup.

The variation in M concerning the air gap is shown in Figure 12 while the alignment is perfect. As expected, when the distance was increased, the mutual inductance decreased. The decrease was initially sharp; almost 40% at 20 mm. The decrease was moderate at 20 mm.

Table 1. Proposed system design parameters.

Parameter	Value
Input voltage (V)	25
Output voltage (V)	25
Output power (W)	50
Frequency (kHz)	85
Airgap (cm)	5
Output current (A)	2.5
C_1 (nF)	49.72
C_2 (nF)	49.72
L_1 (μH)	70.19
L_2 (μH)	70.19
M (μH)	18.83
Q_P	3.96
Q_s	3.39

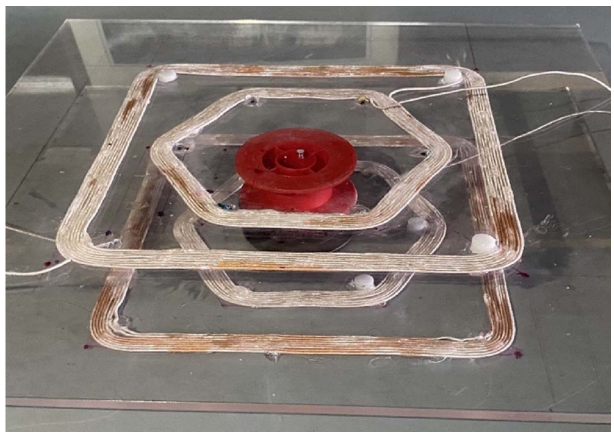

Figure 8. Proposed coil structure.

Table 2. Comparison of self and mutual inductance values with FEA and measurement results.

Method	L (μH)		M (μH)
	Primary	Secondary	
FEA	70.19	70.19	18.83
Measurement	69.1	69.3	19.2
Error (%)	1.5	1.26	1.92

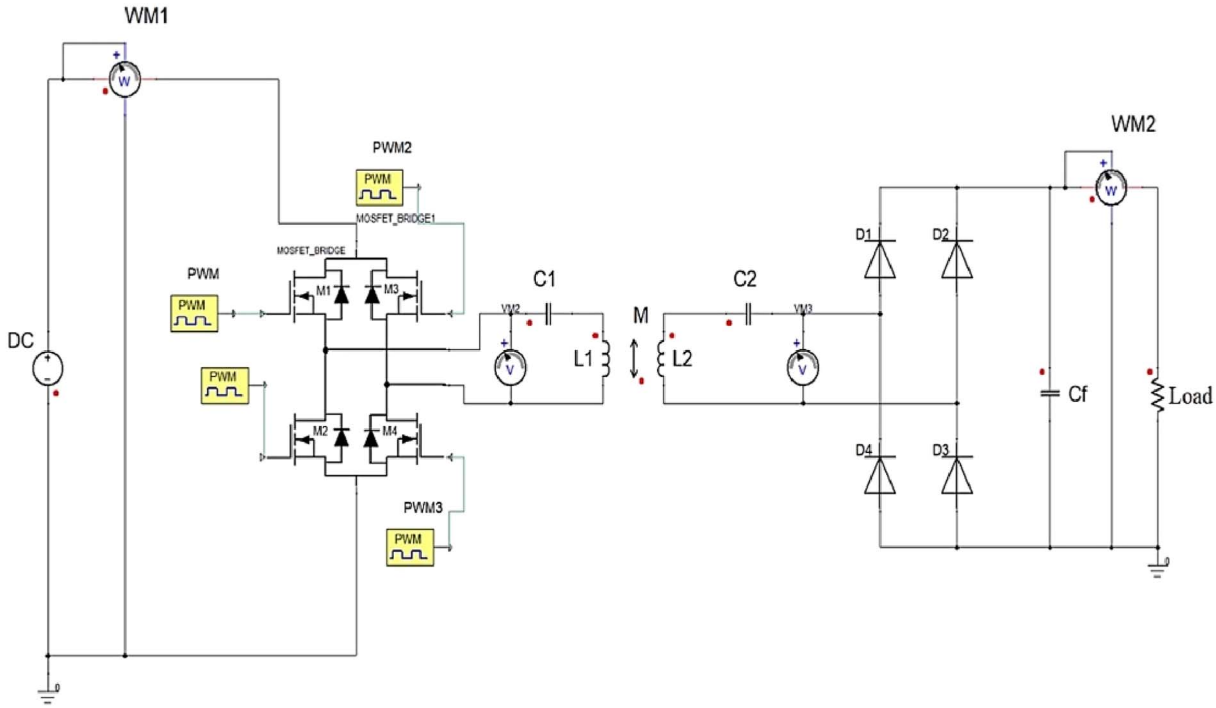

Figure 9. Simulation model of designed WPT system.

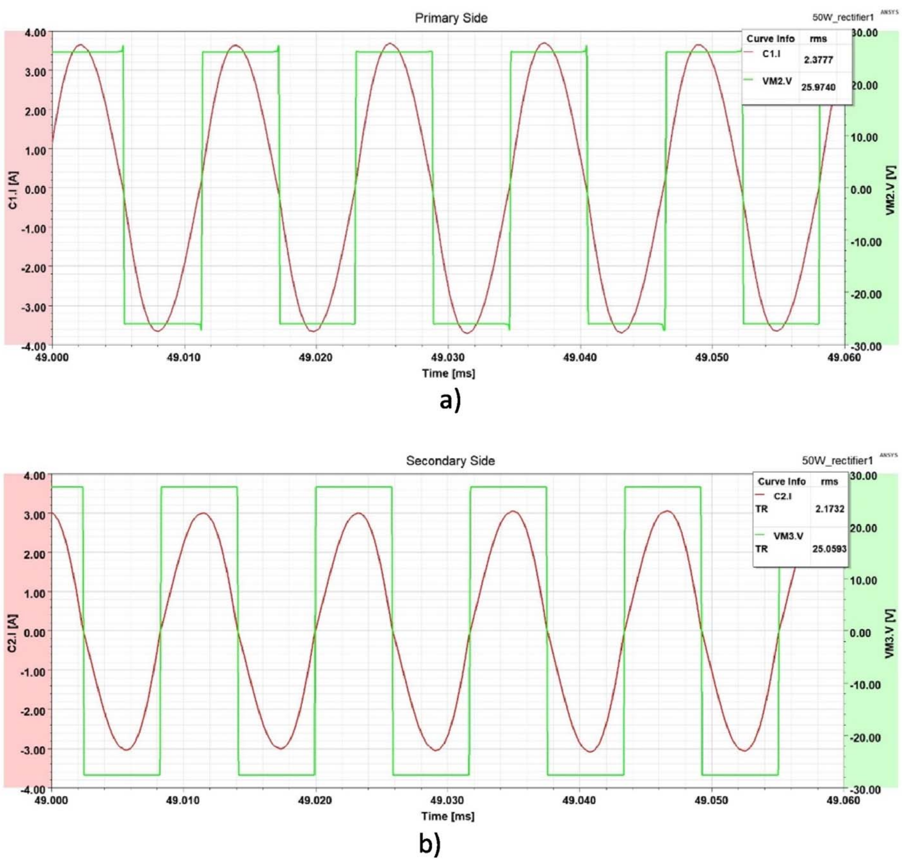

Figure 10. Simulation results. a) Primary, b) Secondary.

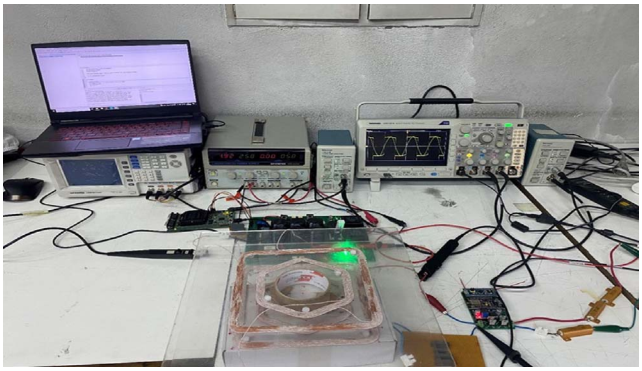

Figure 11. Experimental setup.

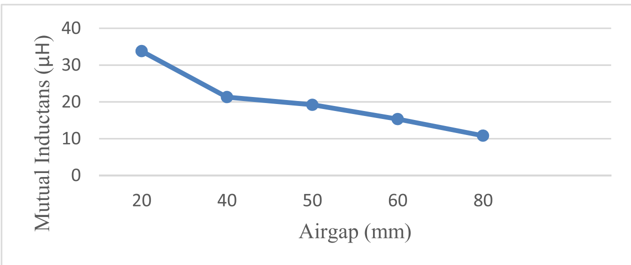

Figure 12. Effect of air gap change on mutual inductance.

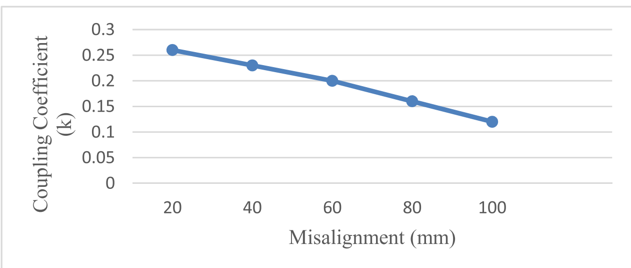

Figure 13. Coupling coefficient change as a result of misalignment in the x-axis while.

Figure 13 shows the effects of misalignment in the x-axis while the air gap is fixed at 5 cm. The secondary coil is shifted so that there is an offset between the centers of the coils of 20, 40, 60, 80, and 100 mm, respectively.

The results of the system when there is misalignment in both the x and y-axis while the air gap is fixed are shown in Figure 14. Figure 15 shows the output power measured in this case. As the results show, although the coupling decreases as the misalignment increases the power is not seriously affected.

According to the measurement results, the efficiency of the proposed WPT structure from the coil to the coil is 93.5%, and the efficiency from the input to the output is 87% due to the losses of the bridge diodes, switching, and copper losses. capacitors of 50 μF were used as compensation capacitors on both sides of the resonant circuit. The currents and voltages on both sides are shown in Figure 16.

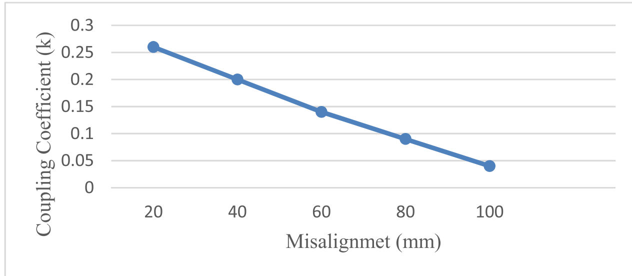

Figure 14. Coupling coefficient change as a result of misalignment both in x-axis and y-axis while the airgap is fixed.

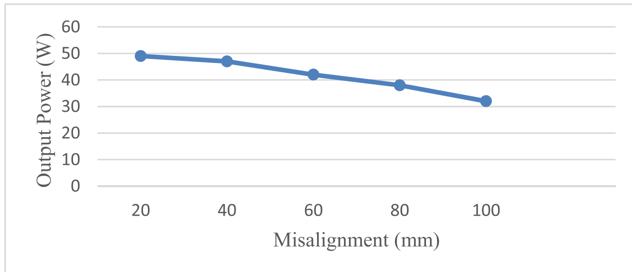

Figure 15. Output power variation as a result of x-axis misalignment.

5 Discussion and conclusions

A hybrid coil design is proposed to enhance the magnetic coupling between the primary and secondary coils and the misalignment tolerance for all ranges of power applications of WPT systems. A 3D model of the proposed and conventional square coil designs was created and analyzed using ANSYS, Maxwell. To perform a fair comparison, some parameters are considered constant for both designs and the performance of the designs has been obtained for different secondary coil positioning. According to the FEA results, the proposed hybrid square-hexagonal structure has a better coupling coefficient value not only for the perfectly aligned but also for the misaligned conditions. When the results are examined, the coupling coefficient value of the proposed coil structure is 0.27 for the perfectly aligned condition, while the coupling coefficient value of the conventional square coil structure is 0.23 which means that the proposed design has a 17% better coupling coefficient value. To determine the accuracy of the proposed coil structure, various tests were conducted for a 50-W WPT system installed in a laboratory environment. As a result of this application, 93.5% efficiency from coil to coil and 87% efficiency from input to output were obtained.

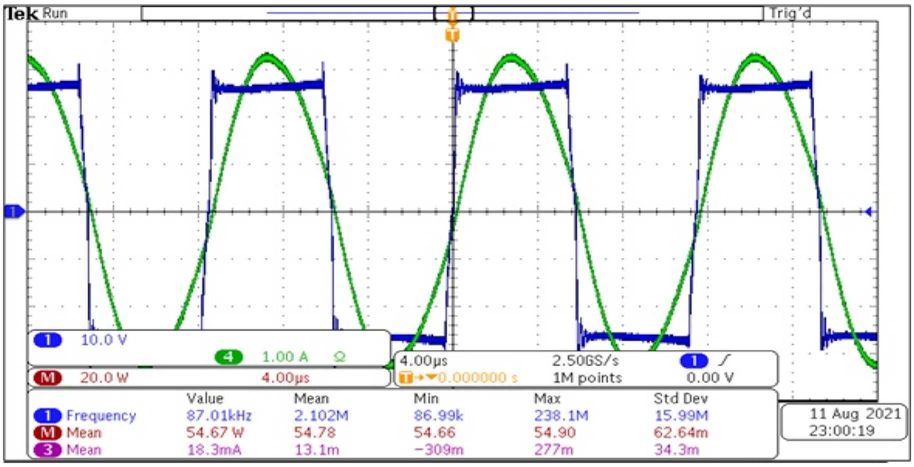

a)

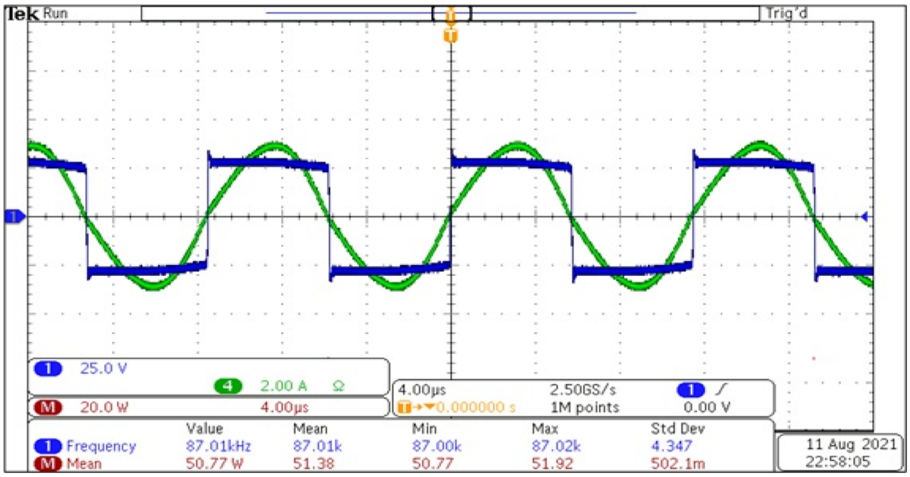

b)

Figure 16. Measured a) Primary, b) Secondary.

Acknowledgments

Not applicable.

Funding

The authors did not receive support from any organization for the submitted work. The authors have no relevant financial or non-financial interests to disclose.

Conflicts of interest

The authors declare that they have no competing interests.

Author contribution statement

AP and EA constructed the targeted system. AP, EA, and MOA analyzed the experimental results and measurements. MTA and YK operate on power electronic boards and circuits. Ap and EA analyses of the FEA simulations. All authors have read and approved the final manuscript.

Ethics approval and consent to participate

Not applicable.

Consent for publication

Not applicable.

References

1 Shladover S.E. (2007) Progressive deployment steps leading toward an automated highway system (AHS), in: *Transportation research record No. 1727*, Transportation Research Board, 2000, Washington, DC, pp. 154–161.

2 Boys J.T., Green A.W. (1994) Inductive power distribution system, ed: Google Patents, 1994.

3 Li S., Mi C.C. (2015) Wireless power transfer for electric vehicle applications, *IEEE J. Emerg. Sel. Top. Power Electron.* **3**, 1, 4–17.

4 Zheng C., Lai J.-S., Chen R., Faraci W.E., Zahid Z.U., Gu B. (2015) High-efficiency contactless power transfer system for electric vehicle battery charging application, *IEEE J. Emerg. Sel. Top. Power Electron.* **3**, 65–74.

5 Liu Z., Chen Z., Li J., Guo Y., Xu B. (2017) A planar L-shape transmitter for a wireless power transfer system, *IEEE Antenn. Wireless Propag. Lett.* **16**, 960–963.
6 Bojarski M., Asa E., Outeiro M.T., Czarkowski D. (2015) Control and analysis of multi-level type multi-phase resonant converter for wireless EV charging, in: *Industrial electronics society, IECON 2015–41st annual conference of the IEEE, 2015*, pp. 005008–005013.
7 Quinn J.C., Limb B.J., Pantic Z., Barr P., Zane R. (2015) Techno-economic feasibly and environmental impact of wireless power transfer roadway electrification, in: *Wireless power transfer conference (WPTC)*, 2015 IEEE, pp. 1–3.
8 Miller J.M., Onar O.C., Chinthavali M. (2015) Primary-side power flow control of wireless power transfer for electric vehicle charging, *IEEE J. Emerg. Sel. Top. Power Electron.* **3**, 147–162.
9 Chinthavali M., Onar O.C., Campbell S.L., Tolbert L. (2015) Integrated charger with wireless charging and boost functions for PHEV and EV applications, in: *Transportation electrification conference and expo (ITEC)*, IEEE, pp. 1–8.
10 Zhang Y., Chen K., He F., Zhao Z., Lu T., Yuan L. (2016) Closed-form oriented modeling and analysis of wireless power transfer system with constant-voltage 135 source and load, *IEEE Trans. Power Electron.* **31**, 472–3481.
11 Chen W., Liu C., Lee C.H., Shan Z. (2016) Cost-effectiveness comparison of coupler designs of wireless power transfer for electric vehicle dynamic charging, *Energies* **9**, 11, 906.
12 Kalwar K.A., Mekhilef S., Seyedmahmoudian M., Horan B. (2016) Coil design for high misalignment tolerant inductive power transfer system for EV charging, *Energies* **9**, 11, 937.
13 Budhia M., Boys J.T., Covic G.A., Huang C.-Y. (2013) Development of a single-sided flux magnetic coupler for electric vehicle IPT charging systems, *IEEE Trans. Industr. Electron.* **60**, 318–328.
14 Covic G.A., Boys J.T. (2013) Modern trends in inductive power transfer for transportation applications, *IEEE J. Emerg. Sel. Top. Power Electron.* **1**, 28–41.
15 Zaheer A., Kacprzak D., Covic G.A. (2012) A bipolar receiver pad in a lumped IPT system for electric vehicle charging applications, in: *IEEE energy conversion congress and exposition (ECCE)*, pp 283–290.
16 Ahmad A., Alam M.S., Chabaan R. (2018) A comprehensive review of wireless charging technologies for electric vehicles, *IEEE Trans. Transport. Electrif.* **4**, 1, 38–63.
17 Budhia M., Covic G.A., Boys J.T. (2011) Design and optimization of circular magnetic structures for lumped inductive power transfer systems, *IEEE Trans. Power Electron.* **26**, 11, 3096–3108.
18 Ongayo D., Hanif M. (2015) Comparison of circular and rectangular coil transformer parameters for wireless power transfer based on finite element analysis, in: *IEEE 13th Brazilian power electronics conference and 1st southern power electronics conference*, pp. 1–6.
19 Budhia M., Covic G., Boys J. (2010) A new IPT magnetic coupler for electric vehicle charging systems, in: *IECON 2010–36th annual conference on IEEE industrial electronics society*, IEEE, pp. 2487–2492.
20 Takanashi H., Sato Y., Kaneko Y., Abe S., Yasuda T. (2012) A large air gap 3 kW wireless power transfer system for electric vehicles, in: *IEEE energy conversion congress and exposition*, pp. 269–274.
21 Aqueel A., Mohammad S.A., Ahmed A.S.M.M. (2019) Design and interoperability analysis of quadruple pad structure for electric vehicle wireless charging application, *IEEE Trans. Transport. Electrif.* **5**, 4.
22 Pries J., Galigekere V.P., Onar O.C., Su G. (2019) A 50 kW three-phase wireless power transfer system using bipolar windings and series resonant networks for rotating magnetic fields, *IEEE Trans. Power Electron.* **35**, 5, 4500–4517.
23 Romlie M.F., Lau K., Zainol M.Z., Abdullah M.F., Kannan R. (2018) Performance of inductive coupled power transfer versus the coil shape, investigation using finite element analysis, *MATEC Web Conf.* **225**, 01017.
24 Castillo-Zamora I.U., Huynh P.S., Vincent D. (2019) Hexagonal geometry coil for a WPT high-power fast charging application, *IEEE Trans. Transport. Electrif.* **5**, 4.
25 Cheng D.K., et al. (1989) *Field and wave electromagnetics*, Pearson Education India, India.
26 Pinuela M., Yates D.C., Lucyszyn S., Mitcheson P.D. (2013) Maximizing DC-to-load efficiency for inductive power transfer, *IEEE Trans. Power Electron.* **28**, 2437–2447.
27 Ameri M.H., Varjani A.Y., Mohamadian M. (2016) A new maximum inductive power transmission capacity tracking method, *J. Power Electron.* **16**, 6, 2202–2211.
28 Xia C., Zhou Y., Zhang J., Li C. (2012) Comparison of power transfer characteristics between CPT and IPT system and mutual inductance optimization for IPT system, *J. Comput.* **7**, 11, 27342741.
29 Agcal A., Bekiroglu K., Ozcira S. (2015) Examination of efficiency based on air gap and characteristic impedance variations for magnetic resonance coupling wireless energy transfer, *J. Magnet.* **20**, 1, 57–61. The Korean Magnetics Society.
30 Zahid Z.U., Zheng C., Chen R., Faraci W.E., Lai J.-S., Senesky M., Anderson D. (2013) Design and control of a single-stage large air-gapped transformer isolated battery charger for wide-range output voltage for EV applications, in: *Proceedings of the IEEE energy conversion congress and exposition*, Denver, CO, USA, pp. 5481–5487.
31 Samanta S., Rathore A.K. (2016). Wireless power transfer technology using full-bridge current-fed topology for medium power applications, *IET Power Electron.* **9**, 9, 19031913.
32 Wang C.-S., Covic G.A., Stielau O.H. (2004). Power transfer capability and bifurcation phenomena of loosely coupled inductive power transfer systems, *IEEE Trans. Ind. Electron.* **51**, 1, 148157.
33 Kosesoy Y., Aydin E., Yildiriz E., Aydemir M.T. (2019) Design and implementation of a 1-kW wireless power transfer system for EV charging, in: *Proceedings of the IEEE 13th international conference on compatibility, power electronics and power engineering*, pp. 1–5.
34 Aydin E., Aydemir M.T.A. (2021) A 1-kW wireless power transfer system for electric vehicle charging with hexagonal flat spiral coil, *Turkish J. Electr. Eng. Comput. Sci.* **29**, 5, 2346–2361. 16p.